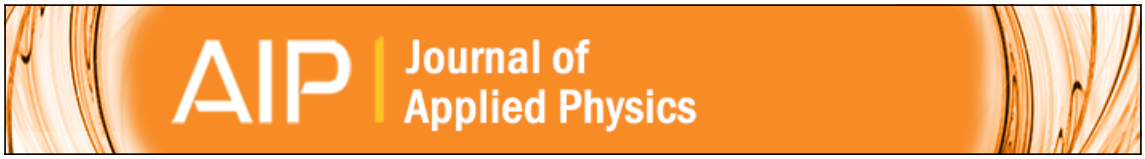

Structural and optoelectronic properties of Gerich hydrogenated amorphous silicongermanium alloys

C. F. O. Graeff and I. Chambouleyron

Citation: Journal of Applied Physics **76**, 2473 (1994); doi: 10.1063/1.357599

View online: http://dx.doi.org/10.1063/1.357599

View Table of Contents: http://scitation.aip.org/content/aip/journal/jap/76/4?ver=pdfcov

Published by the AIP Publishing

Structural and optoelectronic properties of Ge-rich hydrogenated amorphous silicon-germanium alloys

C. F. O. Graeff and I. Chambouleyron
Instituto de Física "Gleb Wataghin," Universidade Estadual de Campinas, Unicamp 13083-970 Campinas, S.P., Brazil

(Received 29 November 1993; accepted for publication 27 April 1994)

In this work the structural and opto-electronic properties of rf sputtered germanium-rich hydrogenated amorphous silicon germanium alloys (a-Si_xGe_{1-x}:H) are presented. It has been found that for $x \leqslant 0.1$, the Si incorporation does not appreciably affect, either the density of localized states in the pseudo-gap, or the structural properties of the films. However the Tauc's optical gap shifts from 1.04 eV ($x=0.0$) to $\approx$1.13 eV ($x=0.1$). A concomitant two orders of magnitude decrease of the dark conductivity is measured, whereas the photoconductivity remains essentially unchanged. In other words, the incorporation of small amounts of Si in the hydrogenated amorphous germanium (a-Ge:H) network produces a noticeable increase of the photosensitivity of the samples. These results are discussed in the framework of present models of amorphous semiconductor alloys.

I. INTRODUCTION

The need of efficient, cheap, and stable materials for the photovoltaic conversion of sunlight has been the main motivation for many research groups investigating new semiconductor compounds. In order to increase the conversion efficiency of solar cells, an appropriate match of the spectral distribution of the solar spectrum and the light absorption in the active layer must be obtained. The deposition technologies of amorphous semiconductors are particularly suited to easily tailor the band gap of alloys. Among the most promising materials to satisfy the efficiency optimization requirements are the hydrogenated alloys of amorphous silicon and germanium (a-Si_xGe_{1-x}:H).[1–3] In these alloys the optical band gap can be easily tailored from $\simeq$1.1 to 1.8 eV by suitably changing the relative content of the elements. It has always been found, however, that the electronic properties of the alloyed films are inferior to those of a-Si:H. The reasons for this deterioration, in terms of midgap density of states (or dangling bond density, N_{DB}) and mobility-lifetime product ($\mu\tau$) of electrons and holes[2–8] are not yet completely understood. It appears that to some extent the degradation of the electronic properties are a consequence of nonoptimized deposition conditions. Up to now, the research effort has mainly concentrated on the optimization of the silicon-rich side of the alloys ($x \geqslant 0.5$), the germanium-rich side remaining almost unexplored.[3,9–11]

In recent years it has been shown that the deposition conditions leading to a-Ge:H films of improved quality are quite different from those normally used to deposit high-quality a-Si:H films.[12,13] In this work we present results on the structural and optoelectronic properties of small band gap a-Si_xGe_{1-x}:H (1.05 eV $< E_g$(Tauc) $<$1.35 eV) films, deposited by the rf sputtering deposition technique. The deleterious effects of Si incorporation in the a-Ge:H network will be analyzed. It will be shown that small ($x \leqslant 0.1$) concentrations of Si do not appreciably affect the density of states (DOS) of a-Ge:H. However, the photosensitivity of the films can be satisfactorily increased.

II. EXPERIMENT

The a-Si_xGe_{1-x}:H samples were deposited by rf co-sputtering pure crystalline targets of Ge and Si, in an atmosphere of Ar and H_2 of high purity (99.997%). The composition was controlled by the relative Si and Ge target areas. Let us remember that under the reported plasma conditions the sputtering yield of Ge is 2.45 times larger than that of Si.[14] The deposition parameters were the following: (a) A total pressure of 1.5×10^{-2} mbar, (b) a H_2 partial pressure of 1.4×10^{-3} mbar, (c) a substrate temperature of 220 °C, (d) a self bias of the powered electrode kept at -640 V. The pressure on the chamber prior to deposition was approximately 10^{-6} mbar. The deposition rate was around 0.1 nm s^{-1}, but decreased slightly with increasing Si concentration. It should be pointed out, however, that the conditions above are not those corresponding to the best a-Ge:H thin films.[13] The composition of the samples was determined by: (1) electron microprobe analysis (EMA) using an electron beam of 15 kV and (2) Rutherford back scattering (RBS) using a 2.2 MeV $^4He^+$ ion from a van de Graaff accelerator. The concentration of bonded hydrogen was obtained from the integrated absorption of the Ge-H and Si-H wagging vibrational mode centered at $\approx$600 cm^{-1}.[15] Infrared spectra were taken in a Fourier transform spectrometer (Perkin–Elmer FT1600) in the 400–4000 cm^{-1} range, on samples grown onto crystalline Si substrates. The sample thickness, the absorption coefficient α (for $\alpha > 500$ cm^{-1}), and the Tauc's optical gap were calculated from the interference fringes of optical transmission spectra.[16] Urbach tails and defect densities were estimated from the absorption coefficient edge and the subgap absorption spectra measured by photothermal deflection spectroscopy (PDS). Samples deposited onto Corning 7059 glass were used to obtain PDS and optical transmission spectra. Dark- and photoconductivity measurements were performed on samples deposited onto glass substrates having evaporated chromium parallel contacts. Photoconductivity measurements were made with chopped light ($\approx$13 Hz) coming from a tungsten halogen lamp (50 W), using the lock-in

 0021-8979/94/76(4)/2473/6/$6.00

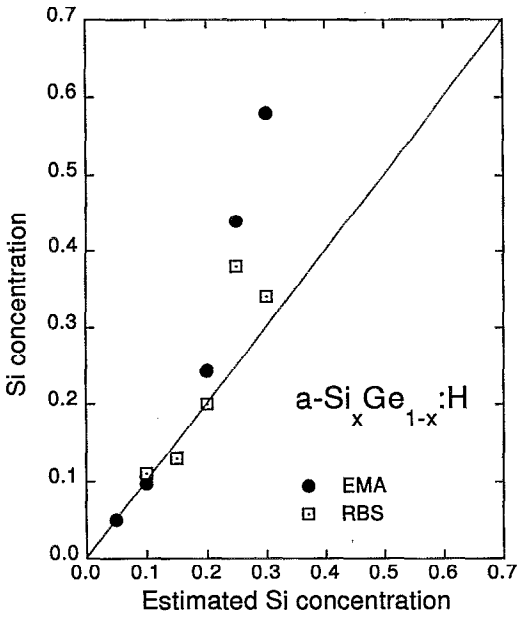

FIG. 1. Si concentration in the a-Si_xGe_{1-x}:H samples measured by electron microprobe analysis (EMA) and Rutherford backscattering (RBS) as a function of the estimated Si concentration from sputtering parameters. The estimated composition was calculated from the Si sputtered area, the total area of the Ge target, and the sputtering yields of Si and Ge.

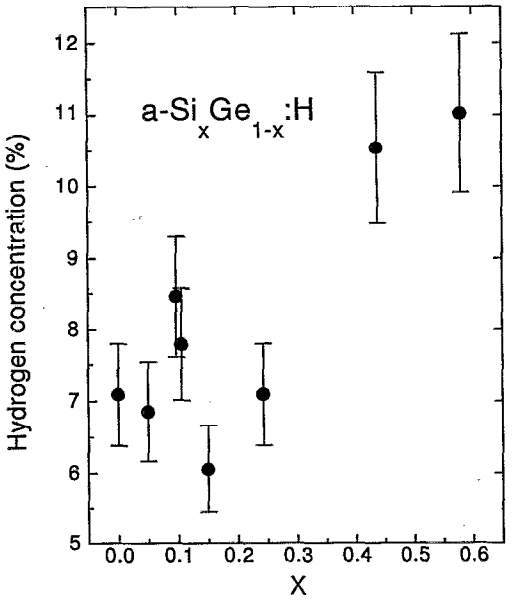

FIG. 2. Hydrogen concentration (%) as a function of Si concentration in the films. Note that for $x>0.25$, the hydrogenation increases from ≈7% to 11%.

technique. The air mass one (AM1) condition was simulated by a 100 mW cm^{-2} heat-filtered light coming from a tungsten halogen lamp. In some cases where higher photon fluxes were necessary, the photoconductivity was measured using the 1.16 eV line of a NdYAg laser.

III. RESULTS AND DISCUSSION

The deposition of amorphous semiconductor alloys by the rf-sputtering technique allows an easy control of the film composition with the additional advantage that solid and gaseous sources may be combined in a single operation. For example, the hydrogen concentration of a-Si:H or a-Ge:H films can be easily controlled by adjusting the hydrogen partial pressure in the chamber during film growth. In the case of co-sputtering two or more different solid targets, the sputtering yields and the relative areas of the materials being co-sputtered are the only information needed to accurately predict the final composition of the sample. Unfortunately, it has not been possible to deposit by rf-sputtering a-Si:H films of the same quality as those produced by plasma enhanced chemical vapor deposition (or glow discharge). Regarding a-Ge:H films, it appears that both methods may produce samples of comparable quality.[12,13]

A series of a-Si_xGe_{1-x}:H films were deposited with silicon concentrations varying from $x=0$ to $x\approx0.6$. The film compositions determined by EMA and RBS were compared to those estimated from the sputtered areas and yields. In the present case a good agreement was found between the three methods for $x\leqslant0.2$ (Fig. 1). However discrepancies between EMA and RBS results were observed for $x>0.2$. The large deviation measured for $x>0.2$ may originate from compositional inhomogeneities. The RBS data correspond typically to an analyzed volume of $1\times0.2\times d$ cm^3 (where d is the thickness of the film, ≈1 μm). In the case of EMA the volume is typically on the order of $1\times1\times1$ μm^3. Thus EMA and RBS measure the composition in a different film volume scale, which may account for the discrepancy found at Si concentrations larger than $x=0.2$. We do not have at the moment a definite explanation for these inhomogeneities appearing at $x>0.2$. But, in support of the above assumption, let us mention that Yang *et al.*[17] have found persistent evidence of compositional inhomogeneity in Si-rich a-Si_xGe_{1-x}:H films. Wind *et al.*[18] determined that microstructure on a 10 nm scale existed in doped, undiluted Si-Ge films, and that it corresponded to Ge-enriched clusters in a silicon enriched matrix. A likely clustering might happen in films having an increase in silicon content. Hereinafter the Si concentration of films will be those measured by EMA.

Hydrogenation plays a major role on the properties of amorphous semiconductors. The hydrogen concentration remains approximately constant at ~7%–8% for $x\leqslant0.25$. For higher Si concentrations it becomes larger, as seen in Fig. 2. This abrupt change in hydrogenation is an indication of a major change in the film structure, in agreement with the evidence of composition inhomogeneities, as discussed above. Another possible explanation comes from the preferential attachment of hydrogen to silicon bonds.[8] We have found that approximately 15% of the Si atoms are bonded to H, whereas the fraction drops to only ≈ 5% for Ge atoms. In the case $x\approx0.2$ the Si-H contribution to the total absorption is less than 3%, i.e., much less than half of the total hydrogen concentration. On the contrary, for $x\approx0.4$ the Si-H contribution increases to 6%, representing more than half of the total hydrogen concentration. In other words, because of the preferential attachment of hydrogen to silicon, the hydrogen concentration in the alloys increases more than

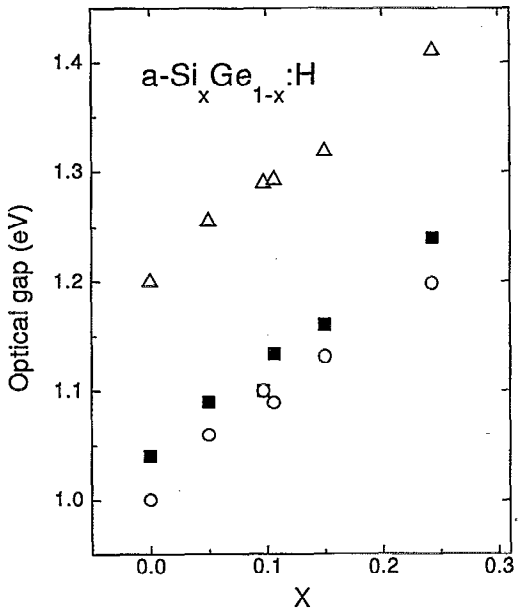

FIG. 3. Optical gap (eV) as a function of silicon concentration in a-Si$_x$Ge$_{1-x}$:H films using three different definitions: (filled squares) Tauc's optical gap E_g, and (open circles) E_{03} and (open triangles) E_{04} corresponding to the photon energy at which the sample's absorption coefficient is 1000 and 10000 cm^{-1}, respectively.

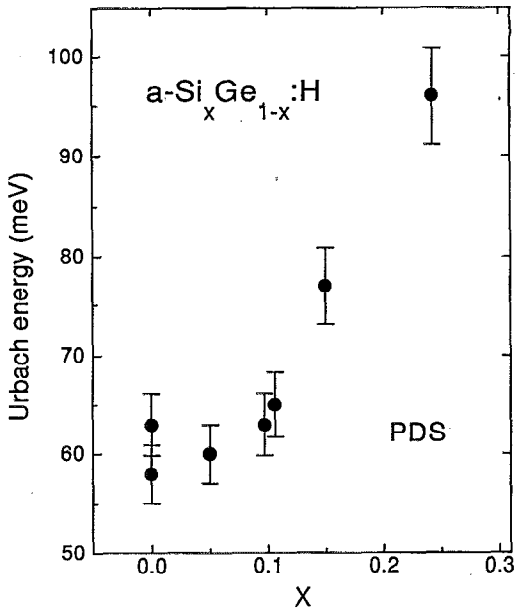

FIG. 4. Urbach tail energy (E_0) as a function of silicon concentration in a-Si$_x$Ge$_{1-x}$:H films.

linearly with increasing silicon content. From the above discussion and to simplify our analysis, the following discussion will only be concerned with samples where $x \leqslant 0.25$. On passing, we would like to mention that neither bending (scissors) of the Si-H$_2$ or Ge-H$_2$ vibration modes were detected in the infrared spectra of the samples, nor oxygen or carbon related absorption peaks, an indication that we have a compact material.[19,20]

In the picture of a molecular orbital representation of the conduction and valence bands, the sp^3 orbitals are split by the bonding interactions to form the valence and conduction bands. Since the split between the bonding and anti-bonding state is larger in Si than in Ge, the introduction of Si atoms in the a-Ge:H network increases the energy gap. In Fig. 3 the optical gap, as defined by the Tauc relation[21]

$$(\alpha h\nu)^{1/2}=B(h\nu-E_g) \tag{1}$$

(where $h\nu$ is the photon energy, B is a constant and E_g is the Tauc's gap) is presented for several samples as a function of the Si fraction. In the same figure the alternative optical gap definitions of E_{04} and E_{03} have also been plotted as a function of alloy composition x. E_{04} and E_{03} corresponds to the photon energy at which the sample's absorption coefficient is 10 000 and 1000 cm^{-1}. It may be seen that the three optical parameters (E_g, E_{04}, E_{03}) depend linearly on x with basically the same slope. The experimental data of E_{04} and E_g obey approximately the following expression:

$$\begin{aligned} E_{04}&=1.21+0.75x, \\ E_g&=1.05+0.75x. \end{aligned} \tag{2}$$

Note that, as discussed in the Introduction, the samples being analyzed here have an E_g between 1.04 and 1.24 eV, a region almost not explored in the literature.[3,9–11]

In Street's description of the amorphous semiconductors electronic density of states,[22] localized states exist between the extended electronic states of the valence band and those of the conduction band. These localized states originate from disorder. Tails of localized states appear near the band edges. There are also coordination defects [dangling bonds, (DBs)] giving electronic states deep in the pseudo-gap. The influence of localized states is apparent in electrical transport, doping, recombination, and many other properties. Thus the electronic properties of amorphous semiconductors are markedly influenced by the presence, distribution, and density of these states. The density of localized states near the valence or the conduction band edge decays exponentially with energy. The valence band (VB) tail density of states is best described by the following relation:

$$N(E)=N_0 \exp(-E/kT_v), \tag{3}$$

where E is the energy measured from the band edge and T_v is a characteristic temperature. Let us assume that the Ge-rich a-Si$_x$Ge$_{1-x}$:H alloys mirror the behavior of a-Si:H alloys, in which the VB-tail is much broader than the conduction band (CB) tail. In this case the Urbach energy or the slope E_0 of the exponential tail of the optical absorption near the fundamental edge, given by:

$$\alpha \propto \exp[(h\nu-E_g)/E_0] \tag{4}$$

mainly describes the VB tail characteristic energy. The Urbach tail characteristic energies of the present a-Si$_x$Ge$_{1-x}$:H alloys as determined PDS are plotted in Fig. 4. From the figure it is clear that for $x \leqslant 0.1$ sharp tails are

found with E_0 roughly constant and equal to 60 meV. E_0 increases rapidly to $\simeq$100 meV for $x>0.1$. The corresponding behavior is detected in electronic transport measurements, as presented next. Another important parameter derived from the PDS spectra is the defect density (N_{DB}). In a previous work,[23] the absorption coefficient at 0.7 eV as measured by PDS was correlated with the DB density (N_{DB}) for a-Ge:H films as determined from electron spin resonance. The calibration constant, $N_{DB}=9\times10^{15}\alpha(0.7\text{ eV})$, was used in the present case to estimate the defect density of the alloys but using, instead of 0.7 eV, the absorption coefficient at (0.7 eV + the increase of the Tauc's optical band gap) as the value to be multiplied by the calibration constant. Using this method, it was found that the defect density stays around 10^{17} cm^{-3} for all samples, a value comparable to the best N_{DB} reported in the literature.[2,3] As the content of Si increases in the a-Ge:H network, the reliability of the above method is expected to decrease, since a different calibration constant is found for a-Si:H ($N_{DB}=2\times10^{16}$ cm^{-3}; $\alpha=1.3$ eV).[24]

It was found that in all $x\leqslant0.1$ a-Si_xGe_{1-x}:H samples the dark conductivity (σ_d) is thermally activated down to at least 200 K and well described by

$$\sigma_d=\sigma_0\exp(-E_a/kT), \tag{5}$$

where σ_0 is the microscopic conductivity, and E_a is the conductivity activation energy. However for $x>0.1$, deviations from this temperature activated behavior were observed at temperatures below 250 K. This is an indication of the contribution of electron hopping between localized states at the Fermi energy,[25] corresponding to an increased defect density close to mid-gap, a N_{DB} increment on alloying not detected through PDS measurements. Thus to explain the apparent contradiction, let us remember that as already pointed out, the procedure used to derive the defect density in the a-Si_x Ge_{1-x}:H alloys may not be appropriate especially for $x\geqslant0.15$. Assuming that the statistical shift of the Fermi energy and the gap shrinkage give negligible contributions,[10] $E_a=E_c-E_F$, where E_c is position of the conduction band mobility edge, and E_F is the Fermi level. In all samples the ratio E_a/E_g was found to be $\approx$ 0.44$\pm$0.02, which indicates that the samples are n type, as expected. The constant ratio E_a/E_g also indicates that the Fermi level is pinned relatively to the CB-mobility edge. Either the Si-DB states are located in the pseudo-gap at the same energy as the Ge-DB, or the Ge-DB are the dominant defects for the alloys being analyzed here. In agreement with previous studies the second assumption seems more plausible to us.[5,7,8,10]

The study of photoconductivity in amorphous semiconductors allows a closer understanding of the recombination process of excess carriers. In its simplest form, the secondary photoconductivity can be expressed as

$$\Delta\sigma_{ph}=\Delta ne\mu, \tag{6}$$

where Δn is the excess photoexcited electron density, μ is the electron mobility, and e the electron charge. It has been assumed that as in a-Si:H, the secondary photoconductivity is basically carried by electrons, since the hole mobility is orders of magnitude smaller than that of electrons.[5] In the

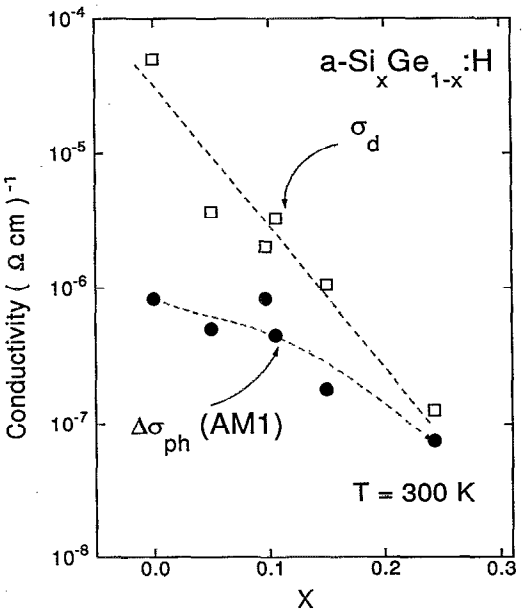

FIG. 5. Dark- (open squares) and photo- (filled circles) conductivity (Ω^{-1} cm^{-1}) as a function of Si concentration in the films. The photoconductivity ($\Delta\sigma_{ph}$) was measured using a tungsten halogen lamp simulating air mass 1 (AM1) conditions.

steady state $\Delta n=G\tau$, where G is the photo-excitation rate and τ is the electron lifetime, and since $G\approx\eta\alpha F(1-R)$, where η is the quantum efficiency, α the absorption coefficient, F the photon flux, and R the reflection coefficient, Eq. (6) can be rewritten as

$$\Delta\sigma_{ph}=\alpha(1-R)Fe\eta\mu\tau. \tag{7}$$

Depending on the recombination kinetics, τ is usually a function of the generation rate. For a purely monomolecular recombination regime, the electrons and holes recombine via deep defects (DB). In this case $\tau\propto N^{-1}$, where N is the density of DB, and $\Delta\sigma_{ph}\propto F$. On the other hand, in the bimolecular recombination regime, electrons and holes recombine by pair annihilation, thus $\tau\propto n^{-1}=G^{-1/2}$, consequently $\Delta\sigma_{ph}\propto\sqrt{F}$. A more detailed discussion on the general solution of the excess carrier rate equations in a semicondutor in which recombination can occur either by bimolecular band-to-band transitions or monomolecular recombination via defects, has been given by Stutzmann *et al.*[26] However, in general it is found experimentally that

$$\Delta\sigma_{ph}\propto F^{\gamma}, \tag{8}$$

where $0.5<\gamma<1.0$. In the present case the γ factor was found to be around 0.8 for all rf sputtered a-Si_xGe_{1-x}:H films. γ was determined using the NdYAg laser. The photon flux density F was varied in the 10^{13} to 10^{17} photons s^{-1} cm^{-2} range. The above experimental result indicates that the dominating recombination regime is monomolecular for all the a-Si_xGe_{1-x}:H alloy series.

In Fig. 5, the room temperature (300 K) dark- and photoconductivity (AM1) are shown as a function of x. In agreement with the results of PDS, the photoconductivity remains

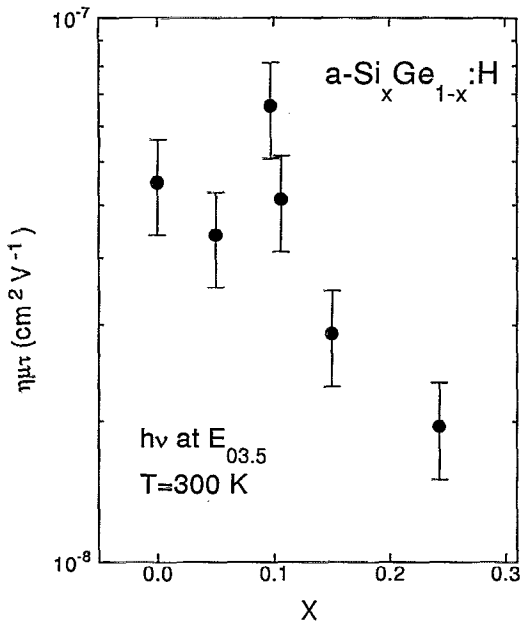

FIG. 6. $\eta\mu\tau$ product ($cm^2\ V^{-1}$) measured at $E_{03.5}$ as a function of Si concentration in a-Si_xGe_{1-x}:H films Note the decrease in the $\eta\mu\tau$ product for $x>0.1$.

approximately constant for $x\leqslant 0.1$, but decreases with increasing x above this value. Figure 5 shows that a clear improvement of the $\Delta\sigma_{ph}/\sigma_d$ ratio is obtained with the introduction of Si in the a-Ge:H network. However, the photoconductivity is still of the same order of magnitude as the dark conductivity.

Since the majority of the photons of an AM1 illumination condition is mainly absorbed near the surface, it is convenient to measure the photoconductivity of a-Si_xGe_{1-x}:H samples under conditions of uniform photogenerated excess carriers. To this aim monochromatic photoconductivity measurements were made. The photon energy was adjusted to the $E_{03.5}$ condition ($h\nu$ at which $\alpha=10^{3.5}\ cm^{-1}$) with a photon flux of $\approx 10^{15}$ photons $cm^{-2}\ s^{-1}$. Under these conditions the light is almost homogeneously absorbed in the bulk and the carrier generation rate remains small. With the help of Eq. (7) $\eta\mu\tau$ was calculated and the results shown in Fig. 6. Their behavior is similar to that obtained under AM1 irradiation. For samples having $x>0.1$, the $\eta\mu\tau$ product decreases. This is consistent with the increase in N_{DB} determined from the dark conductivity for $x>0.1$. Moreover, PDS measurements indicate that the VB-tail is broadened for $x>0.1$, see Fig. 4. Thus, most probably, the decrease in the $\eta\mu\tau$ product is due to both a decrease in the mobility related to the broadening of the tails and to a decrease in τ due to a higher defect density. Unfortunately the present data cannot separate both contributions to the decrease in the $\eta\mu\tau$ product. On the other hand, the $\eta\mu\tau$ products of the present a-Si_xGe_{1-x}:H samples are comparable to those recently reported.[3–5]

IV. SUMMARY AND CONCLUSION

The opto-electronic properties of rf-sputtered germanium rich amorphous silicon germanium alloys (a-Si_xGe_{1-x}:H, $x\leqslant 0.25$) have been studied. It has been found that the incorporation of silicon in the a-Ge:H network up to $x\approx 0.1$, neither appreciably affects the density of deep defects (N_{DB}) of a-Ge:H nor the Urbach tail characteristic energy (E_0). In the present samples $E_0\approx 60$ meV and $N_{DB}\approx 10^{17}$ cm^{-3}. Thus the photoconductivity and/or the $\eta\mu\tau$ product remain approximately constant ($\eta\mu\tau\approx 6\times 10^{-8}\ cm^2\ V^{-1}$). However, the pseudo-gap increases with Si incorporation (from 1.04 to $\approx$1.1 eV) and, consequently, the dark conductivity at room temperature decreases by two orders of magnitude. Better photosensitivities are thus obtained in the alloys.

A preferential attachment of hydrogen to Si was confirmed and found to be a factor of 3 higher than in a-Ge. Our results indicate that Ge-DB is the predominant defect in the whole alloy range. For $x>0.1$, an increase in E_0 and N_{DB} is accompanied by a decrease in the $\eta\mu\tau$ product.

ACKNOWLEDGMENTS

The authors are indebted to Professor C. A. Ribeiro, UNICAMP, for EMA measurements, to Professor F. L. Freire Jr., Pontificia Universidade Catolica do Rio de Janeiro, for RBS measurements, and Dr. D. Comedi for a critical reading of the manuscript. The authors would like to thank Professor M. Stutzmann, Walter Schotky Institute, Technical University of Munich for many helpful discussions, and aid with the PDS measurements. This work was partially supported by the Fundação de Amparo à Pesquisa do Estado de São Paulo (FAPESP), Brazil.

[1] D. E. Carlson, Philos. Mag. B **63**, 305 (1991).
[2] W. Paul, R. A. Street, and S. Wagner, J. Electron. Mater. **22**, 39 (1993).
[3] W. Paul, J. H. Chen, E. Z. Liu, A. E. Wetsel, and P. Wickboldt, J. Non-Cryst. Solids **164–166**, 1 (1993).
[4] F. Karg, W. Krühler, M. Möller, and K. v. Klitzing, J. Appl. Phys. **60**, 2016 (1986).
[5] S. Aljishi, Z. E. Smith, and S. Wagner, in *Amorphous Silicon ana Related Materials*, edited by H. Fritzsche (World Scientific, Singapore, 1988), p. 887.
[6] C. E. Nebel, M. Schubert, H. C. Weller, G. H. Bauer, and W. H. Bloss, in Proceedings of the 8th ECPVSEC, Reidel, Dordrecht, 1988, p. 919.
[7] W. Fuhs and F. Finger, J. Non-Cryst. Solids **114**, 387 (1989).
[8] M. Stutzmann, R. A. Street, C. C. Tsai, J. B. Boyce, and S. E. Ready, J. Appl. Phys. **66**, 569 (1989).
[9] V. Chu, J. P. Conde, D. S. Shen, and S. Wagner, Appl. Phys. Lett. **55**, 262 (1989).
[10] D. Della Sala, C. Reita, G. Conte, F. Galluzzi, and G. Grillo, J. Appl. Phys. **67**, 814 (1990).
[11] T. Drüsedau and B. Schröder, Appl. Phys. Lett. **61**, 566 (1992).
[12] W. Paul, J. Non-Cryst. Solids **137&138**, 803 (1991).
[13] I. Chambouleyron, J. Phys.: Condens. Matter **5**, A73 (1993).
[14] R. V. Stuart, *Vacuum Technology, Thin Films, and Sputtering. An Introduction* (Academic, Orlando, FL 1983).
[15] C. J. Fang, K. J. Grunz, L. Ley, M. Cardona, F. J. Demond, G. Muller, and S. Kalbitzer, J. Non-Cryst. Solids **35&36**, 255 (1980).
[16] R. Swanepoel, J. Phys. E: Sci. Instrum. **16**, 1214 (1983).
[17] L. Yang, J. Newton, and B. Fieselmann, Proc. Mat. Res. Soc. **149**, 497 (1989).
[18] J. Wind, G. Krotz, V. Petrova-Koch, G. Muller, and P. Deimel, J. Non-Cryst. Solids **114**, 531 (1989).
[19] G. A. N. Connell and J. R. Pawlik, Phys. Rev. **13**, 787 (1976).
[20] W. Beyer, J. Herion, H. Wagner, and U. Zastrow, Philos. Mag. B **63**, 269 (1991).

[21] J. Tauc, R. Grigorovici, and A. Ancu, Phys. Status Solidi **15**, 627 (1966).
[22] R. A. Street, *Hydrogenated Amorphous Silicon* (Cambridge University Press, Cambridge, UK, 1991).
[23] C. F. O. Graeff, M. Stutzmann, and K. Eberhardt, Philos. Mag. B **69**, 387 (1994).
[24] M. S. Brandt, A. Asano, and M. Stutzmann, in Mater. Res. Soc. Symp. Proc., Vol. 297, edited by E. A. Schiff, M. J. Thompson, A. Madan, K. Tanaka, and P. G. LeComber (MRS, Pittsburgh, 1993), p. 201.
[25] N. F. Mott and E. A. Davis, *Electronic Processes in Non-Crystalline Materials* (Oxford University Press, Oxford, 1971).
[26] M. Stutzmann, J. Nunnenkamp, M.S. Brandt, and A. Asano, Phys. Rev. Lett. **67**, 2347 (1991).